

# RECURSIVE PROPORTIONAL-FEEDBACK AND ITS USE TO CONTROL CHAOS IN AN ELECTROCHEMICAL SYSTEM<sup>†</sup>

P. PARMANANDA, R. W. ROLLINS, P. SHERARD

*Condensed Matter and Surface Sciences Program,  
Department of Physics and Astronomy, Ohio University, Athens, Ohio 45701-2979*

and

H. D. DEWALD

*Condensed Matter and Surface Sciences Program,  
Department of Chemistry, Ohio University, Athens, Ohio 45701-2979*

## ABSTRACT

We report the successful application of a simple recursive proportional-feedback (RPF) algorithm to control chemical chaos observed during the electrodisolution of a rotating copper disk in a sodium acetate/acetic acid buffer. The RPF method is generally applicable to the control of chaotic systems that are highly dissipative and adequately described by one-dimensional maps of a single variable. The successive minima of the measured anodic current generate a return map that is used to implement the control strategy and the anodic potential is the control parameter. Unstable periodic orbits of period one and period two are stabilized by applying small perturbations ( $\approx 0.05\%$ ) to the anodic potential on each cycle of the periodic oscillation. Experimental evidence is presented to indicate why the RPF method was necessary in this system and the theoretical robustness of the algorithm is discussed.

## 1. Introduction

Two experiments were recently reported describing the control of autonomous oscillatory chemical systems in the chaotic regime. Petrov, Gáspár, Masere, and Showalter<sup>1</sup> stabilized periodic orbits in the Belousov-Zhabotinsky reaction and we

---

<sup>†</sup>Published in “Proceedings of the 2nd Conference on EXPERIMENTAL CHAOS” edited by W. Ditto, L. Pecora, S. Vohra, M. Shlesinger, and M. Spano (World Scientific, River Ridge NJ, 1995) pp 304–316.

recently reported<sup>2</sup> the first experiment to control chaotic oscillations in an electrochemical cell. In controlling the electrochemical cell we found it necessary, in general, to use the recursive proportional-feedback (RPF) algorithm recently developed by Rollins, Parmananda, and Sherard<sup>3</sup>. The RPF algorithm is simple to apply and is generally applicable to highly dissipative systems that are well described by a one-dimensional Poincaré return map of a single measured variable. In this paper we report the further use of the RPF algorithm to stabilize both period-1 and period-2 orbits in the electrochemical system. We also present experimental evidence that suggests why we found it necessary to use the new RPF method instead of the simple proportional feedback method suggested by Petrov, Peng, and Showalter<sup>4</sup> and by Hunt<sup>5</sup> that often works for systems well described by a one-dimensional return map. Finally, we briefly discuss the robustness of the RPF method. This discussion is based on an analysis of the RPF method in terms more akin to standard control theory<sup>6</sup> as described recently for the general high dimensional system by Romeiras, Grebogi, Ott, and Dayawansa<sup>7</sup>. This approach treats the experimental system (described by a one-dimensional return map of a single variable) together with a linear recursive control strategy applied to a single control parameter as a discrete two-dimensional system. The desired periodic orbit is a fixed point of the two-dimensional map. The range of acceptable control conditions is determined by the requirement that the fixed point remain stable. The RPF control strategy<sup>3</sup> makes the fixed point superstable.

## 2. Experimental System

The experimental system was a three-electrode electrochemical cell set up to study the potentiostatic electrodisolution of copper in an acetate buffer electrolyte solution of sodium acetate and acetic acid. The experimental setup and the general electrochemical behavior of the system is described in some detail by Dewald, Parmananda, and Rollins<sup>8,9</sup>. Figure 1 is a schematic diagram of the system.

The anode was a rotating copper disk (5 mm diameter) shrouded in a cylinder of Teflon. The supporting electrolyte solution was a mixture of 60 parts glacial acetic acid to 35 parts 2M sodium acetate. The potential of the anode was measured relative to a saturated calomel reference electrode (SCE) and the cathode was a 2.5 cm<sup>2</sup> platinum foil disk. The emf of the circuit was continuously adjusted by a potentiostat to maintain the desired set value of the anodic potential (the potential between the anode and the reference electrode). The anodic potential was used as our control parameter. Time series data was collected by measuring the anodic current at 20 ms intervals using a 12 bit A/D converter interfaced to a computer. The period for the current oscillations in the chaotic states used in these experiments ranged from 2 to 4 sec so that the time between data points in the time series is small compared to the typical period of the oscillations. The set point for the anodic potential was controlled by the computer through a D/A converter with the smallest increment of the control voltage being 0.1 mV.

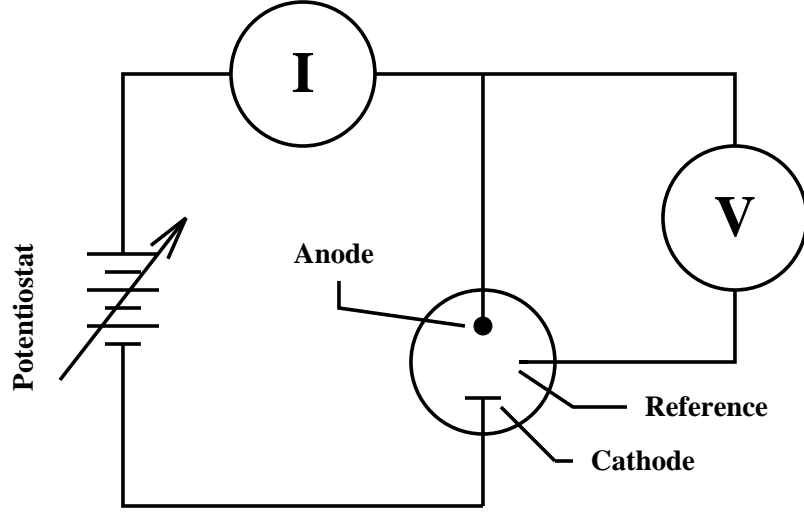


Figure 1: Schematic representation of the three-electrode electrochemical cell.  $V$  is the anodic potential and  $I$  is the anodic current. The potentiostat adjusts the emf to hold  $V$  at the desired set value.

### 3. Control Method

The RPF control strategy<sup>3</sup> was used to stabilize both period-1 and period-2 orbits within chaotic attractors measured by a time series of the anodic current. A Poincaré section was taken at the time when the anodic current goes through a minimum. A one-dimensional return map was constructed from the sequence of current minima where  $I_n$  is the current minimum at the beginning of the  $n$ th Poincaré cycle. The value of the anodic potential during the  $n$ th cycle is  $V_n = V + \delta V_n$ . According to the RPF algorithm, control is established by adding an increment to the anodic potential during the  $n$ th cycle given by<sup>2,3</sup>

$$\delta V_n = K(I_n - I_F) + R \delta V_{n-1}, \quad (1)$$

where  $I_F$  is the unstable fixed point of the target orbit for the return map obtained for a time series taken at  $V = V_0$ . The value of  $I_F$  and the constants  $K$  and  $R$ , are determined from a precontrol experimental procedure carried out using an interactive computer program for data acquisition and display.

The precontrol procedure is described in detail in references<sup>2,3</sup>. Firstly, the fixed point  $I_F$  and the slope,  $\mu$ , of the one-dimensional return map was determined by a least square fitting of the displayed return map ( $I_n$  versus  $I_{n-1}$ ) for a sequence of current minima collected in the neighborhood of the desired fixed point with the anodic potential held constant at  $V = V_0$ . Secondly, a sequence of current minima

were collected and displayed as a return map while the anodic potential is changed back and forth between two values;  $V_n = V_0$  for  $n$  odd and  $V_n = V_0 + \Delta V$  for  $n$  even. The value of  $\Delta V > 0$  was chosen to be about the size of the maximum  $\delta V_n$  used later during control. If the system is sufficiently dissipative, as our electrochemical system was, the resulting return map consists of two curves called the *up* and *back* maps formed from alternate  $(I_{n-1}, I_n)$  pairs with  $n$  odd and even respectively. The shift in the fixed point per unit  $\Delta V$  is measured by least squares fitting for the *up* and *back* maps giving  $g_u$  and  $g_b$  respectively. The values of  $K$  and  $R$  were then calculated using the RPF relations<sup>3</sup>

$$K = \frac{\mu^2}{(\mu - 1)(\mu g_u + g_b)}, \quad R = \frac{-\mu g_b}{(\mu g_u + g_b)}. \quad (2)$$

Typically these control constants,  $K$  and  $R$ , could be determined within 10–20 minutes (corresponding to approximately 200 cycles of the experimental return map) from the start of data acquisition.

With these control constants available, the control algorithm was initiated. The anodic potential was changed according to the RPF algorithm of Eq. 1 whenever a minimum of the anodic current,  $I_n$ , came within about 0.2 mA of the measured fixed point  $I_F$ .

## 4. Results and Discussion

### 4.1. Control of period-1 and period-2 orbits

Examples of the successful stabilizing of period-1 and period-2 orbits are shown in Fig. 2. The rotation rate for the copper disk anode was  $\omega = 2670$  rpm, the anodic potential with control off was  $V_0 = 0.724$  V, and the values of the RPF proportionality constants were  $K = -5.0$  mV/mA and  $R = -0.3$  for the period-1 control shown in Fig. 2a. For the period-2 control shown in Fig. 2b,  $\omega = 2160$  rpm,  $V_0 = 0.745$  V,  $K = -5.0$  mV/mA, and  $R = 0.21$ . As described in reference 2, we chose a region of parameter space where the electrochemical system exhibits a sequence of periodic mixed mode oscillations separated by bands of chaotic behavior as a function of anodic potential. The period-1 control was done while in the chaotic region between a period-1 state with large amplitude oscillations only and a period-2 state with one large amplitude oscillation followed by one small oscillation. We were unsuccessful in controlling on the period-2 oscillation in this chaotic band. Successful control of a period-2 state was attained in the chaotic band between the period-2 (one large–one small) and period-3 (one large and two small) mixed mode oscillations. We found that control of the period-2 orbit was much more difficult than the period-1. This is partially because the period is about twice as long (about 5 sec) and the feedback corrections are made just once each cycle. Thus the system can drift further away from its fixed point before the next feedback correction is calculated and applied.

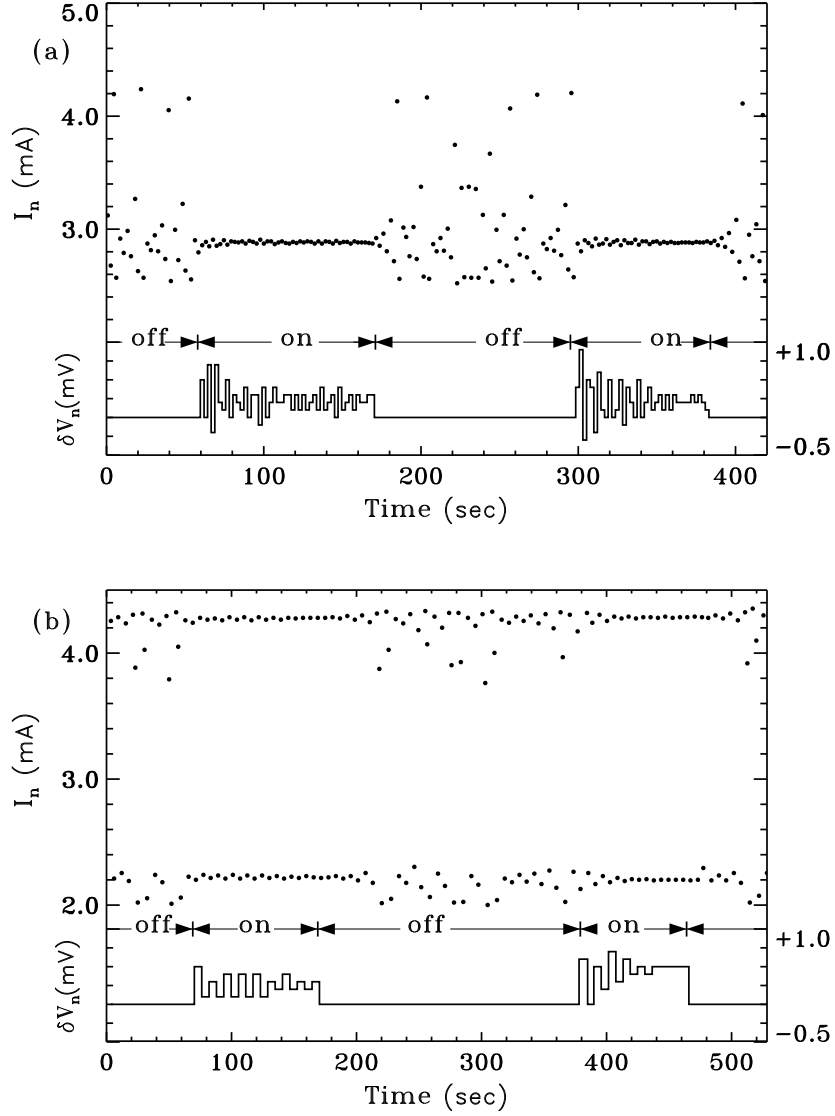


Figure 2: The minima in anodic current plotted over a time period during which the control algorithm is switched on and off twice. The perturbations added to the anodic potential to maintain control are shown in the bottom graph. (a) shows period-1 control and (b) shows period-2 control.

The corresponding return maps for the two cases are shown in Fig. 3 while Fig. 4 and 5 show the chaotic attractors and controlled periodic orbits reconstructed from the time series of the anodic current using a two-dimensional time delay embedding.

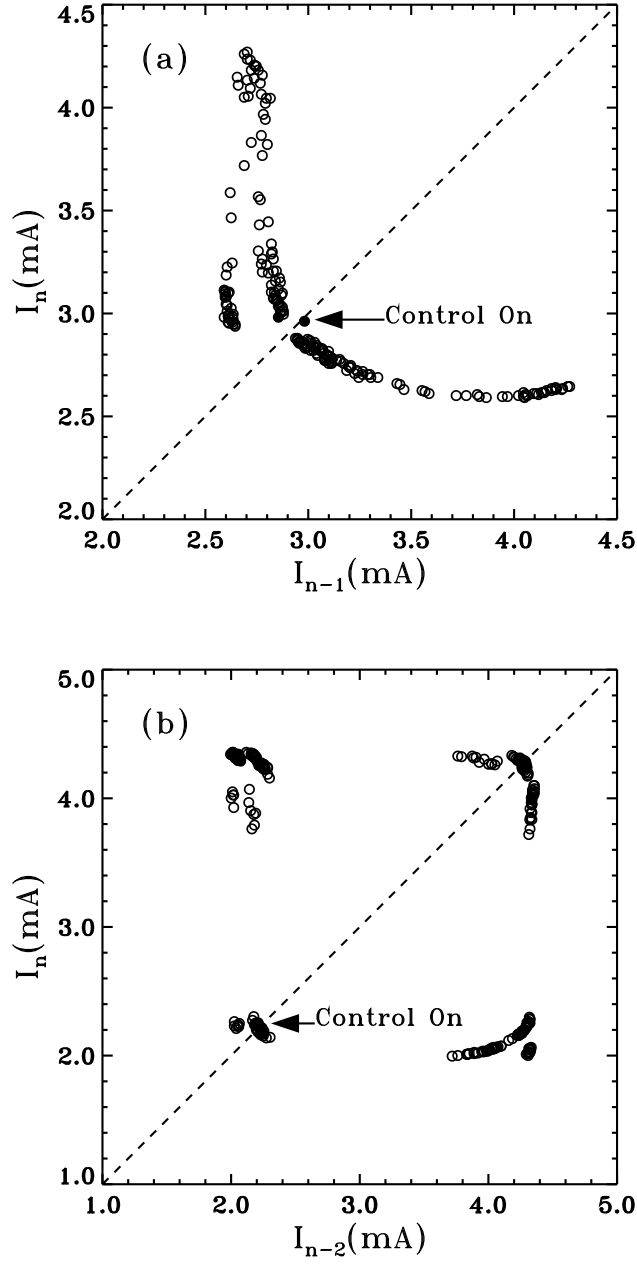


Figure 3: (a) The first iterate return map (open circles) obtained from the sequence of current minima for the chaotic state shown in Fig. 2a. The superimposed filled circles are the minima in the anodic current while the control algorithm was implemented. (b) the corresponding second-iterate return map for the period-2 case shown in Fig. 2b.

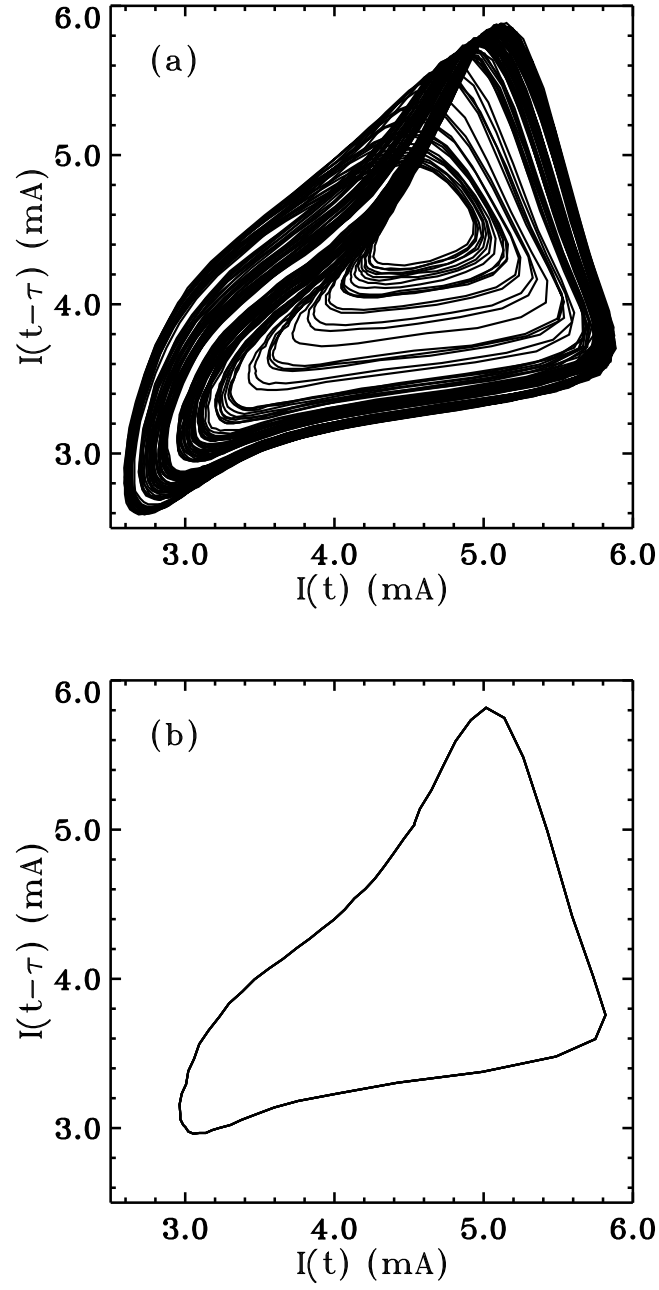


Figure 4: (a) The two-dimensional time delay embedding with  $\tau = 120$  msec showing the chaotic attractor for the situation shown in Figs. 2a and 3a. (b) the corresponding period-1 trajectory with control on.

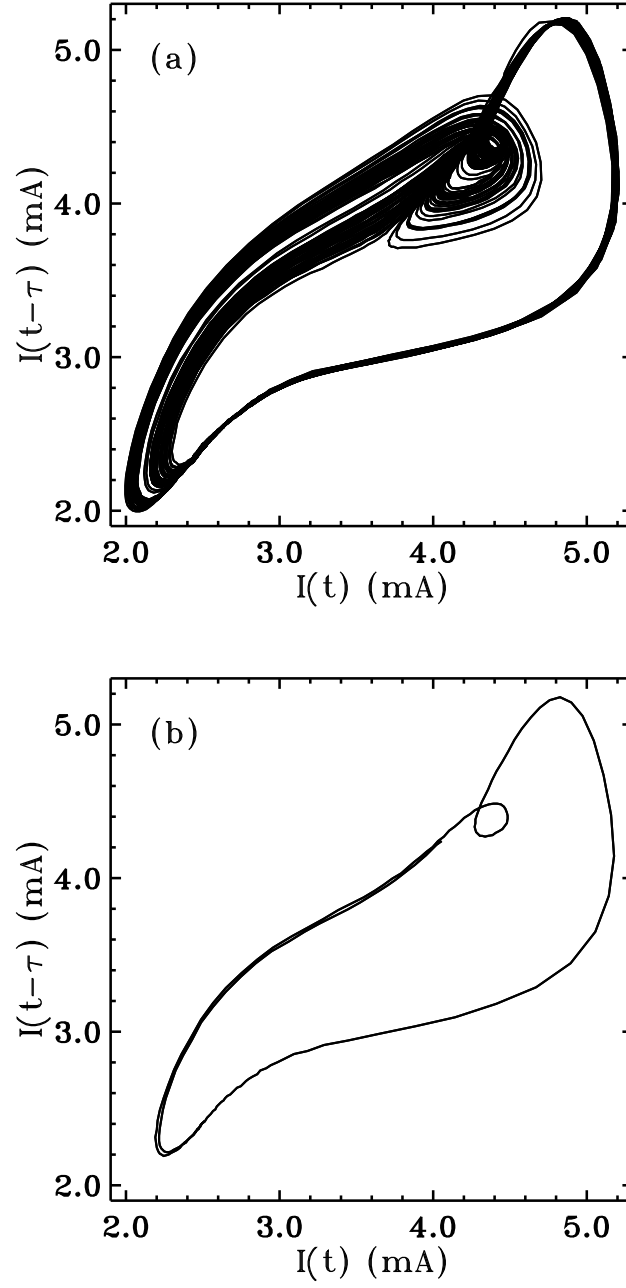


Figure 5: (a) The two-dimensional time delay embedding with  $\tau = 120$  msec showing the chaotic attractor for the situation shown in Figs. 2b and 3b. (b) the corresponding period-2 trajectory with control on.



#### 4.2. Why use RPF method

Feedback methods used to control chaos as discussed in this paper are most closely related to the algorithm first proposed by Ott, Grebogi, and Yorke (OGY)<sup>10</sup>. The original OGY method required the measurement of two system variables at the Poincaré surface (in a three dimensional system) to determine the appropriate feedback for control. However, many experimental situations (such as that described in this paper) donot easily allow the measurement of more than one variable. It was recently found<sup>3,11,12</sup> that the original OGY method must be modified to apply to the situation where single time series data is used. In general, this requires nontrivial modification of the algorithm and makes the prescribed change in the control parameter on the  $n$ th cycle depend on the changes that were made on previous cycles. It was shown in reference 3 that in highly dissipative systems this reduces to a simple recursive algorithm where the change on the  $n$ th cycle depends only on the change made on the  $(n - 1)$ th cycle as indicated in Eq. 1. Furthermore, it was shown that the recursive term goes to zero ( $R = 0$ ) if the attractor (in the neighborhood of the fixed point at the Poincaré section) does not shift in the direction normal to its plane in state space when small changes are made in the control parameter.

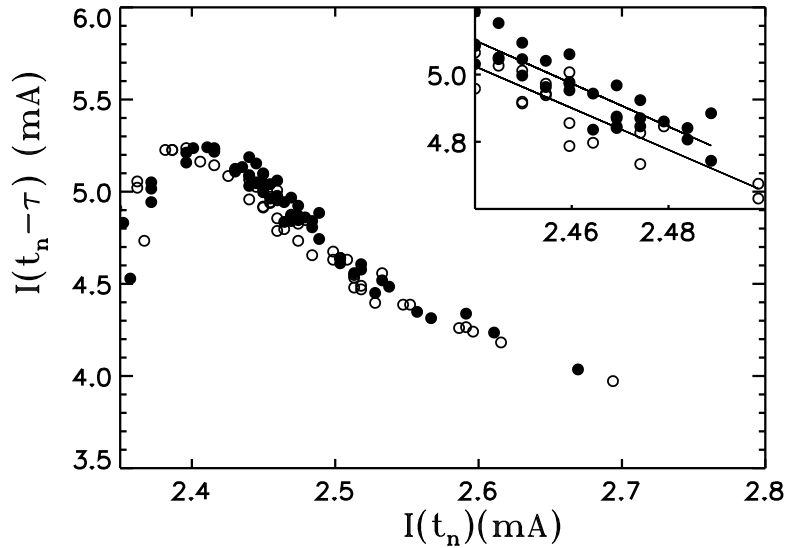


Figure 6: Poincaré sections reconstructed using time delay embedding of the measured time series of the anodic current. The anodic current is minimum at times  $t_n$  and  $\tau = 600$  msec. The open and closed circles are for values of the anodic potential that differ by 4 mV.

Figure 6 shows the Poincaré section of the reconstructed attractor in a delay coordinate embedding for the electrochemical cell at parameter values where we used RPF to control on a period-1 orbit. The time  $t_n$  is the time when the anodic current goes through the  $n$ -th minimum near the period-1 orbit. Two sets of data are shown with the anodic potential,  $V$ , held constant in each case. The open circles are for  $V = 0.720$  V and the closed circles for  $V = 0.724$  V. This figure showing experimental data should be compared with Fig. 1b of reference 3. While the observed experimental shift in the Poincaré section is small, there is clear evidence that a shift is present.

#### 4.3. Theoretical robustness of RPF method

We have found in our experimental work that there is often a rather large range in the values of the RPF proportionality constants  $K$  and  $R$  that will still be effective in controlling the system. This is fortunate since it allows us to make estimates of  $K$  and  $R$  from just a few experimental points in the neighborhood of the desired fixed point during the precontrol phase of the experiment. Here, we briefly derive the RPF equations for  $K$  and  $R$  using methods of control theory<sup>6,7</sup> in order to shed light on the theoretical robustness of the RPF method.

We start with the general 1D return-map equation (Eq. 2 from reference 3)

$$X_{n+1} = f(X_n; p_{n-1}, p_n), \quad (3)$$

where the notation is that used in reference 3,  $X_n$  is the value of the measured variable at the start of the  $n$ th Poincaré cycle and  $p_n$  is the value of the control parameter during the  $n$ th cycle. For control on a period-1 orbit, we are interested in the natural dynamics of the system described by Eq. 3 near the fixed point,  $X_F$ , of the period-1 orbit for  $p = p_0$ ;  $X_F = f(X_F, p_0, p_0)$ . To first order in  $\delta X_n = (X_n - X_F)$ ,  $\delta p_{n-1}$ , and  $\delta p_n$ , we have

$$\delta X_{n+1} = \mu \delta X_n + w \delta p_{n-1} + v \delta p_n, \quad (4)$$

where  $\mu = \partial f(X_F, p_0, p_0) / \partial X_n$ ,  $w = \partial f(X_F, p_0, p_0) / \partial p_{n-1}$ , and  $v = \partial f / \partial p_n$ .

In reference 3, the RPF algorithm is obtained by using the optimum possible strategy of choosing  $\delta p_n$  such that the system is brought to the fixed point as quickly as possible, namely two Poincaré cycles. Taking  $\delta X_{n+2} = 0$  and  $\delta p_{n+1} = 0$ , then the first and second iterate of Eq. (4) gives the recursive control algorithm Eq. 1 with  $R$  and  $K$  given by

$$K = -\frac{\mu^2}{(\mu v + w)}, \text{ and } R = -\frac{\mu w}{(\mu v + w)}. \quad (5)$$

As shown in reference 3,  $w = (1 - \mu)g_b$  and  $v = (1 - \mu)g_u$ , and Eqs. 2 are equivalent to Eqs. 5.

Here we take a different approach. We *assume* there is a bilinear relationship between  $\delta p_n$  and  $(\delta X_n, \delta p_{n-1})$

$$\delta p_n = H \delta X_n + G \delta p_{n-1}, \quad (6)$$

where  $H$  and  $G$  are constants yet to be determined. Equations 4 and 6 form a two-dimensional discrete map describing the full control system including both the dynamics of the nonlinear system and the recursive feedback control strategy. The two-dimensional map is put in more conventional form if we shift the  $n$  labels on the  $p_n$  by 1. This can be accomplished by defining a new parameter,  $\delta\hat{p}_n = \delta p_{n-1}$ . Substitution into Eqs. 4 and 6 gives

$$\delta X_{n+1} = \mu \delta X_n + w \delta\hat{p}_n + v \delta\hat{p}_{n+1} \quad (7)$$

$$\delta\hat{p}_{n+1} = H \delta X_n + G \delta\hat{p}_n. \quad (8)$$

The conventional 2D map is formed by substituting Eq. 8 into the last term of Eq. 7 giving

$$\begin{bmatrix} \delta X_{n+1} \\ \delta\hat{p}_{n+1} \end{bmatrix} = \tilde{M} \begin{bmatrix} \delta X_n \\ \delta\hat{p}_n \end{bmatrix}, \quad (9)$$

where

$$\tilde{M} = \begin{bmatrix} \mu + vH & w + vG \\ H & G \end{bmatrix}. \quad (10)$$

The full control system defined by Eq. 9 has a fixed point at  $\delta X_n = \delta\hat{p}_n = 0$ . The control system will produce the desired control if this fixed point is stable. The parameters  $\mu$ ,  $v$ , and  $w$  are determined by the dynamics of the system near the fixed point and we are free to adjust  $H$  and  $G$ . For successful feedback control, the values of  $H$  and  $G$  must be chosen so that the fixed point of Eq. 9 is stable.

The stability of the fixed point is determined by the magnitude of the eigenvalues of  $\tilde{M}$ :

$$\lambda_{1,2} = \frac{-\text{Tr}\tilde{M} \pm \sqrt{(\text{Tr}\tilde{M})^2 - 4\text{Det}\tilde{M}}}{2}, \quad (11)$$

where  $\text{Tr}\tilde{M} = \mu + vH + G$  and  $\text{Det}\tilde{M} = \mu G - wH$ . The fixed point will be stable if

$$|\lambda_1| < 1 \text{ and } |\lambda_2| < 1. \quad (12)$$

Equations 11 and 12 put conditions on  $H$  and  $G$  such that the control strategy will work.

The best values of  $H$  and  $G$  would make  $\lambda_1 = \lambda_2 = 0$  and the fixed point of the control system becomes superstable. The superstable condition is satisfied if  $H = H^*$  and  $G = G^*$  where

$$\text{Tr}\tilde{M} = 0 = \mu + vH^* + G^* \quad (13)$$

$$\text{Det}\tilde{M} = 0 = \mu G^* - wH^*. \quad (14)$$

The values of  $H^*$  and  $G^*$  that satisfy Eqs. 13 and 14 are

$$H^* = -\frac{\mu^2}{(\mu v + w)}, \text{ and } G^* = -\frac{\mu w}{(\mu v + w)}. \quad (15)$$

Equations 15 are identical to Eqs. 5 for the RPF algorithm with  $K \equiv H^*$  and  $R \equiv G^*$  and we have shown that the RPF algorithm forms a superstable control system. Of course, it is not necessary to have the optimum values for  $K$  and  $R$  for the control to be successful and there is a range of values satisfying the stability conditions of Eqs. 11 and 12.

Finally, if we substitute  $H = H^*$  and  $G = G^*$  into  $\tilde{M}$ , then the map describing the superstable control system becomes

$$\delta X_{n+1} = \frac{1}{(\mu + w)}(\mu \delta X_n + w^2 \delta \hat{p}_n) \quad (16)$$

$$\delta \hat{p}_{n+1} = \frac{1}{(\mu + w)}(-\mu^2 \delta X_n - \mu v \delta \hat{p}_n). \quad (17)$$

Iterating these equations once shows explicitly that, for the superstable RPF control conditions,  $\delta X_{n+2} \equiv 0$  and  $\delta \hat{p}_{n+2} \equiv 0$  for *any* starting values of  $(\delta X_n, \delta \hat{p}_n)$ . Of course,  $\delta X_n$  and  $\delta \hat{p}_n$  must be small enough so that the linearization of the dynamics about  $X_F$  is valid.

## 5. Acknowledgements

We thank Alan Markworth at Battelle, Columbus for his continued thoughtful comments and suggestions on this project. We have also benefited from discussions with Don Weekley, Gregg Johnson, Andreas Rhode, Markus Löcher, and Earle Hunt at Ohio University regarding the experiment and the subtleties of nonlinear dynamics and chaos control. This work was supported in part by a Battelle subcontract of the Electric Power Research Institute (EPRI) research project contract RP2426-25 and by Ohio University Research Challenge Grant RC89-107.

## 6. References

1. V. Petrov, V. Gáspár, J. Masere, and K. Showalter, *Nature*, **361** (1993) 240.
2. P. Parmananda, P. Sherard, R. W. Rollins, and H. D. Dewald, *Phys. Rev.* **E47**, (1993) R3003.
3. R. W. Rollins, P. Parmananda, and P. Sherard, *Phys. Rev.* **E47**, (1993) R780.
4. V. Petrov, B. Peng, and K. Showalter, *J. Chem. Phys.* **96**, (1992) 7506.
5. E. R. Hunt, *Phys. Rev. Lett.* **67**, (1991) 1953.
6. K. Ogata, *Control engineering*, Second Ed. (Prentice-Hall, Englewood Cliffs, NJ, 1990).
7. F. J. Romeiras, C. Grebogi, E. Ott, and W. P. Dayawansa, *Physica D* **58**, (1992) 165.

8. H. D. Dewald, P. Parmananda, and R. W. Rollins, *J. Electroanal. Chem.* **306**, (1991) 297.
9. H. D. Dewald, P. Parmananda, and R. W. Rollins, *J. Electrochem. Soc.* **140**, (1993) 1969.
10. E. Ott, C. Grebogi, and J. A. Yorke, *Phys. Rev. Lett.* **64**, (1990) 1196.
11. U. Dressler and G. Nitsche, *Phys. Rev. Lett.* **68**, (1992) 1.
12. D. Auerbach, C. Grebogi, E. Ott, and J. Yorke, *Phys. Rev. Lett.* **69**, (1992) 3479.